IFIC/97–06
FTUV/97–06
HD-THEP-96-55
hep-ph/9702276

Bottom quark mass and α_s from the Υ system

Matthias Jamin[1] **and Antonio Pich**[2]

[1] *Institut für Theoretische Physik, Universität Heidelberg,*
Philosophenweg 16, D-69120 Heidelberg, Germany

[2] *Departament de Física Teòrica, IFIC, CSIC – Universitat de València,*
Dr. Moliner 50, E–46100 Burjassot, València, Spain

(February 1997)

Abstract

The mass of the bottom quark and the strong coupling constant α_s are determined from QCD moment sum rules for the Υ system. Two analyses are performed using both the pole mass M_b as well as the mass m_b in the $\overline{MS}$ scheme. In the pole-mass scheme large perturbative corrections resulting from coulombic contributions have to be resummed. In the $\overline{MS}$ scheme this can be avoided by an appropriate choice for the renormalization scale. For the bottom quark mass we obtain $M_b = 4.60 \pm 0.02\,\mathrm{GeV}$ and $m_b(m_b) = 4.13 \pm 0.06\,\mathrm{GeV}$. Our combined result from both determinations for the strong coupling is $\alpha_s(M_Z) = 0.119 \pm 0.008$.

1 Introduction

The Upsilon system constitutes a rich source of information about the strong interaction dynamics. The bottom quark mass is sufficiently heavy for a non-relativistic description to be a good starting point to analyze the quark-antiquark forces. Thus, potential models — including relativistic corrections — have been successfully used to understand the spectroscopy of the corresponding mesonic bound states [1–3]. At the same time, the small size of the hadronic system makes possible to attempt a short-distance approach. At the relevant energy scale, α_s is small enough to allow (at least for the lowest levels) a well-grounded quantum field theory analysis with perturbative QCD tools, including non-perturbative corrections through the Operator Product Expansion (OPE) [4]. While the coulombic part of the $b\bar{b}$ potential is obviously related to the static piece of the gluon-exchange interaction, a systematic short-distance investigation provides a better understanding of the remaining terms in the heavy quark potential, in terms of fundamental QCD parameters [5–15].

The short-distance description in terms of quarks and gluons is specially well suited for inclusive quantities, where no reference to a particular hadronic bound state is needed. The vacuum polarization $\Pi(q^2)$ induced by the heavy-quark vector current $\bar{b}\gamma_\mu b$ is then a key ingredient to investigate the $J^P = 1^-$ $b\bar{b}$ states. Its imaginary part can be experimentally determined from the $e^+e^- \to b\bar{b}$ cross-section:

$$R_b(s) \;\equiv\; Q_b^2\, R(s) \;\equiv\; \frac{\sigma(e^+e^- \to b\bar{b})}{\sigma(e^+e^- \to \mu^+\mu^-)} \;=\; 12\pi Q_b^2\, \mathrm{Im}\,\Pi(s+i\epsilon)\,. \qquad (1.1)$$

On the other side, $\Pi(q^2)$ can be calculated theoretically within the OPE. To keep our equations more general, let us consider the vector current $j_\mu(x) = (\bar{Q}\gamma_\mu Q)(x)$, $Q(x)$ being a heavy quark field of mass M, specifically the bottom quark in our case:

$$\Big(q_\mu q_\nu - g_{\mu\nu} q^2\Big)\,\Pi(q^2) \;=\; i \int dx\, e^{iqx}\, \langle\, T\{\, j_\mu(x)\, j_\nu(0)\}\,\rangle\,. \qquad (1.2)$$

Throughout this work, M corresponds to the pole of the perturbatively renormalized propagator, whereas the running quark mass in the $\overline{MS}$ scheme [16] renormalized at a scale μ will be denoted by $m(\mu)$.

Using a dispersion relation the nth derivative of $\Pi(s)$ at $s = 0$ can be expressed

in terms of the nth integral moment of $R(s)$:

$$\mathcal{M}_n \;\equiv\; \frac{12\pi^2}{n!}\left(4M^2\,\frac{d}{ds}\right)^n \Pi(s)\bigg|_{s=0} \;=\; (4M^2)^n \int\limits_0^\infty ds\,\frac{R(s)}{s^{n+1}}\,. \tag{1.3}$$

For later convenience, the moments $\mathcal{M}_n$ are defined to be dimensionless quantities. In addition, it will prove useful to express the moments $\mathcal{M}_n$ in terms of integrals over the variable $v \equiv \sqrt{1-4M^2/s}$,

$$\mathcal{M}_n \;=\; 2\int\limits_0^1 dv\, v(1-v^2)^{n-1} R(v)\,. \tag{1.4}$$

Under the assumption of quark-hadron duality, the moments $\mathcal{M}_n$ can either be calculated theoretically in renormalization group improved perturbation theory, including non-perturbative condensate contributions, or can be obtained from experiment. In this way, hadronic quantities like masses and decay widths get related to the QCD parameters α_s, m_b and condensates.

For large values of n, the moments become dominated by the threshold region. Therefore, they are very sensitive to the heavy quark mass. This fact has been exploited since the very first QCD analyses of charmonium and bottomium [4, 17–23] to extract rather accurate values of m_c and m_b. More recently, it has been suggested by Voloshin [24] that the large-n moments can also be used to get a precise determination of α_s from the existing data on Υ resonances.

The perturbative calculation of the moments contains powers of $\alpha_s\sqrt{n}$ [17,18, 25], which correspond to the coulombic contributions; they are associated with the near-threshold quark-antiquark configurations at typical velocity $v \sim 1/\sqrt{n}$, so that $\alpha_s\sqrt{n} \sim \alpha_s/v$ is the familiar Coulomb parameter. At large n these coulombic $(\alpha_s\sqrt{n})^k$ terms should be explicitly summed up to assure a reasonable convergence of the perturbative series. By the same token, this large-n behaviour implies a big sensitivity to the value of α_s [24].

In ref. [24] the large-n moments $\mathcal{M}_n$ have been studied with a non-relativistic expansion in powers of $1/n$. Fitting the $\mathcal{O}(1/n)$ contribution from the sum rules, the analysis of the moments $n = 8$, 12, 16 and 20 gave the result: $M_b = 4827 \pm 7\,\text{MeV}$ and $\alpha_s^{\overline{\text{MS}}}(M_Z) = 0.109 \pm 0.001$. The quoted errors are claimed to include the experimental uncertainties and the theoretical uncertainty due to subleading $1/n$ terms [24].

The reasoning of ref. [24] looks indeed very suggestive. The large-n moments are dominated by the first Υ resonance. Thus, one is actually starting with

a confined bound state. In spite of that, our ability to make an explicit sum of the coulombic contributions allows to make an impressive determination of the perturbative coupling. Obviously, an accurate analysis of the theoretical uncertainties is called for.

The analysis of ref. [24] was performed at $\mathcal{O}(\alpha_s)$, i.e., only the $\mathcal{O}(1)$ and $\mathcal{O}(\alpha_s)$ perturbative contributions to the correlator $\Pi(q^2)$ were included. Therefore, the scale and scheme dependence of α_s was not under control. Adopting the $\overline{\rm MS}$ scheme, the running of α_s was included in the Coulomb potential, and used to fix the scale of the coulombic contributions. For the remaining short-distance perturbative corrections the BLM prescription [26] was used to justify the choice $\mu = e^{-11/24} M_b$. Given that, the quoted uncertainty in the final α_s determination looks rather unrealistic.

In order to make a more reliable analysis one needs to know the size of the higher-order perturbative corrections. Fortunately, the $\mathcal{O}(\alpha_s^2)$ contributions to the correlator $\Pi(q^2)$ have been studied recently [27–31]. Although a complete analytical calculation of these corrections is still not available, the present information is good enough to perform an accurate analysis of the moments $\mathcal{M}_n$.

In this paper, we present a detailed study of the relevant moments, using all the information on $\Pi(q^2)$ that we are aware of. From the present experimental data we determine the numerical values of the bottom quark mass and the strong coupling. Moreover, we perform a thorough analysis of the associated uncertainties.

The resulting values of $\alpha_s(M_Z)$ and M_b are found to be less precise than what was claimed in ref. [24]. Nevertheless, they still constitute rather accurate determinations. The value of the strong coupling constant turns out to be in excellent agreement with the more precise measurements obtained from the τ hadronic width [32–35] or from $Z \to$ hadrons data [36]. Previous claims [24, 37] that low-energy determinations of α_s result in lower $\alpha_s(M_Z)$ values than higher-energy ones are thus unfounded. On the other side, our analysis of the Υ system provides the most precise determination of the bottom quark mass today.

The known perturbative contributions to the moments are given in Section 2 and the Coulomb resummation is performed in Section 3. The non-perturbative corrections are discussed in Section 4. Section 5 contains the phenomenological parameterization, extracted from the present data. The numerical analysis is presented in Sections 6 and 7, which use the *pole mass* and *modified minimal subtraction* schemes, respectively. A short conclusion is finally given in Section 8.

2 Perturbation theory

In perturbation theory the vacuum polarization $\Pi(s)$ can be expanded in powers of the strong coupling constant,

$$\Pi^{pt}(s) \;=\; \Pi^{(0)}(s) + a\,\Pi^{(1)}(s) + a^2\,\Pi^{(2)}(s) + \ldots\,, \tag{2.1}$$

with $a \equiv \alpha_s/\pi$. Analogously, expansions for $R^{pt}(v)$ and $\mathcal{M}_n^{pt}$ can be written.

For the first two terms, analytic expressions are available [38, 39]. Here, we only give $R^{(0)}(v)$ and $R^{(1)}(v)$. The corresponding formulae for $\Pi^{(0)}(s)$ and $\Pi^{(1)}(s)$ can for example be found in refs. [40, 41].

$$R^{(0)} \;=\; \frac{3}{2}\,v(3-v^2)\,, \tag{2.2}$$

$$\begin{aligned} R^{(1)} \;=\;& 2(1+v^2)(3-v^2)\Big[\,4\mathrm{Li}_2(p) + 2\mathrm{Li}_2(-p) + \ln(p)\Big(\,\ln(1+p) + 2\ln(1-p)\Big)\Big] \\ & - 4v(3-v^2)\Big(\,\ln(1+p) + 2\ln(1-p)\Big) \\ & - \frac{1}{4}\,(1-v)(33-39v-17v^2+7v^3)\ln(p) + \frac{3}{2}\,v(5-3v^2)\,, \end{aligned} \tag{2.3}$$

where $p \equiv (1-v)/(1+v)$ and $\mathrm{Li}_2(z)$ is the dilogarithmic function [42]. The expression for $R^{(1)}$ implicitly includes a factor $C_F = 4/3$.

Using the integral representation (1.4) for $\mathcal{M}_n$, one finds the following expressions for the moments:

$$\mathcal{M}_n^{(0)} \;=\; 3(n+1)\,\mathrm{B}(5/2, n)\,, \tag{2.4}$$

$$\begin{aligned} \mathcal{M}_n^{(1)} \;=\;& \mathrm{B}(5/2, n)\,\Bigg\{\,(2n+3)\,\mathcal{A}_n + n\,\mathcal{A}_{n+1} - 4n + 12 \\ & + \frac{6}{n} + \frac{2}{(n+1)} - \frac{4}{(n+2)} - \frac{6}{(n+3)}\,\Bigg\}\,, \end{aligned} \tag{2.5}$$

with

$$\begin{aligned} \mathcal{A}_n \;=\;& \frac{4}{3}\,\Bigg\{\,1 - \frac{1}{2n} - \frac{3}{(n+1)} - \frac{3}{2(n+2)} \\ & + \left(\frac{1}{n} + \frac{1}{(n+1)}\right)\sum_{k=1}^{n+1}\left[\,\frac{(n+2)\,\mathrm{B}(1/2,k)}{k\,\mathrm{B}(1/2,n)} - \frac{3}{k} + \frac{2}{(2k-1)}\,\right]\Bigg\}\,, \end{aligned} \tag{2.6}$$

and $\mathrm{B}(x,y)$ being Euler's Beta function. The first order moments $\mathcal{M}_n^{(1)}$ are in agreement with the result found by Generalis [40].

The second-order vacuum polarization $\Pi^{(2)}(s)$ is still not fully known analytically. However, the method of Padé approximants has been recently exploited to calculate $\Pi^{(2)}$ numerically, using available results at high energies ($s \to -\infty$), analytical results for the first seven moments $\mathcal{M}_i^{(2)}$ for $i = 1, \ldots, 7$ and the known threshold behaviour $R^{(2)}(v)$ for $v \to 0$ [27–29]. Following the lines of ref. [29], it is convenient to split $\Pi^{(2)}$ according to the colour factors,

$$\Pi^{(2)} \;=\; C_F^2\,\Pi_A^{(2)} + C_A C_F\,\Pi_{NA}^{(2)} + C_F T n_l\,\Pi_l^{(2)} + C_F T\,\Pi_F^{(2)}\,, \tag{2.7}$$

and to treat the four different contributions separately, because they exhibit different behaviour at threshold. $\Pi_A^{(2)}$ and $\Pi_{NA}^{(2)}$ contain the pure gluonic contributions; the first term is already present in an abelian theory, whereas $\Pi_{NA}^{(2)}$ is characteristic of the non-abelian aspects of QCD. The contributions $\Pi_l^{(2)}$ and $\Pi_F^{(2)}$ arise from diagrams with internal light and heavy quark loops respectively.[1] The spectral function $R_l^{(2)}(v)$ is known analytically and $R_F^{(2)}(v)$ receives contributions from a two-particle cut with threshold at $2M$ which is known analytically and a four-particle cut with threshold at $4M$ which can be calculated numerically from a two-dimensional integral [30, 31]. These results can be used to check the reliability of the Padé approximation for the moments. We shall not repeat the technicalities of the calculation of the $\Pi_X^{(2)}$, but refer the reader to ref. [29] for details.

In table 1, we give the first twenty moments $\mathcal{M}_n^{(0)}$, $\mathcal{M}_n^{(1)}$ and $\mathcal{M}_n^{(2)}$, as well as the four contributions to $\mathcal{M}_n^{(2)}$ separately. The first seven moments for $\mathcal{M}_{X,n}^{(2)}$ correspond to the analytic expressions of ref. [29], whereas the moments for $n \geq 8$ are our results obtained from the Padé approximants. In the case of $\mathcal{M}_{A,n}^{(2)}$ the values arise from a [5/4] approximant, and the moments $\mathcal{M}_{NA,n}^{(2)}$, $\mathcal{M}_{l,n}^{(2)}$ and $\mathcal{M}_{F,n}^{(2)}$ were calculated from [4/4] approximants because the constant contribution to $\Pi^{(2)}$ in the limit $v \to 0$ is unknown. To check the stability of our results and thus the reliability of the Padé approximation, either different Padé approximants using the full set of information can be calculated, e.g. [4/5] or [6/3] in the case of $\mathcal{M}_{A,n}^{(2)}$, or Padé approximants with one order less can be constructed by removing one datum. For $\mathcal{M}_{A,n}^{(2)}$ and $\mathcal{M}_{NA,n}^{(2)}$ the largest change is found if the seventh moment is removed as an input datum. In particular, $\mathcal{M}_{A,20}^{(2)}$ changes by 0.002 and $\mathcal{M}_{NA,20}^{(2)}$ by 0.0003. The moments $\mathcal{M}_{l,n}^{(2)}$ and $\mathcal{M}_{F,n}^{(2)}$ can also be calculated from the available results for $R_l^{(2)}$ and $R_F^{(2)}$ [30, 31]. In the case of $\mathcal{M}_{F,n}^{(2)}$, for $n \geq 8$,

[1] With respect to the bottom quark, we consider the up, down, strange and charm quarks to be massless.

n	$\mathcal{M}_n^{(0)}$	$\mathcal{M}_n^{(1)}$	$\mathcal{M}_{A,n}^{(2)}$	$\mathcal{M}_{NA,n}^{(2)}$	$\mathcal{M}_{l,n}^{(2)}$	$\mathcal{M}_{F,n}^{(2)}$	$\mathcal{M}_n^{(2)}$
1	2.4000	12.1481	11.4197	15.9696	-5.2627	1.6358	71.2368
2	1.0286	7.9822	14.3850	14.1999	-4.8914	0.6010	69.7300
3	0.6095	6.0448	15.0503	12.1448	-4.2652	0.3373	64.1861
4	0.4156	4.8899	15.0403	10.5729	-3.7595	0.2238	59.1538
5	0.3069	4.1158	14.7923	9.3710	-3.3623	0.1627	54.9238
6	0.2387	3.5585	14.4586	8.4283	-3.0453	0.1252	51.3801
7	0.1926	3.1370	14.1001	7.6699	-2.7871	0.1003	48.3813
8	0.1596	2.8067	13.7427	7.0464	-2.5727	0.0827	45.8120
9	0.1351	2.5406	13.3977	6.5244	-2.3917	0.0698	43.5843
10	0.1163	2.3214	13.0696	6.0804	-2.2368	0.0599	41.6318
11	0.1015	2.1377	12.7599	5.6980	-2.1025	0.0521	39.9043
12	0.0896	1.9815	12.4685	5.3648	-1.9850	0.0459	38.3628
13	0.0799	1.8468	12.1945	5.0718	-1.8811	0.0409	36.9772
14	0.0718	1.7296	11.9369	4.8118	-1.7886	0.0367	35.7233
15	0.0650	1.6267	11.6945	4.5796	-1.7057	0.0331	34.5821
16	0.0592	1.5354	11.4661	4.3706	-1.6309	0.0301	33.5379
17	0.0542	1.4541	11.2505	4.1816	-1.5629	0.0276	32.5780
18	0.0499	1.3810	11.0468	4.0097	-1.5010	0.0254	31.6919
19	0.0461	1.3150	10.8539	3.8527	-1.4443	0.0234	30.8707
20	0.0428	1.2552	10.6709	3.7086	-1.3921	0.0217	30.1070

Table 1: One-, two- and three-loop perturbative contributions for the first twenty moments $\mathcal{M}_n$.

the moments we are interested in, the contribution of the four-particle cut can be neglected, and it is sufficient to consider the analytically available expressions for the two-particle cut. The agreement with the twentieth moments $\mathcal{M}_{l,20}^{(2)}$ and $\mathcal{M}_{F,20}^{(2)}$ as calculated from the Padé approximants is better than 10^{-6} in both cases. Thus for all moments under consideration the uncertainty is below 0.02%, being completely negligible for our application. We conclude that the method of Padé approximation works sufficiently well to predict the moments up to at least $n = 20$.

Generally, the moments $\mathcal{M}_n^{(2)}$ depend on the renormalization scheme and scale

for the strong coupling constant. The values presented in table 1 correspond to $a(M)$ in the $\overline{MS}$ scheme and a renormalization scale $\mu_a = M$. If the scale μ_a is varied, the moments change according to

$$\mathcal{M}_n^{(2)}(\mu_a) \;=\; \mathcal{M}_n^{(2)}(M) + \beta_1 \mathcal{M}_n^{(1)} \ln \frac{\mu_a}{M}\,. \tag{2.8}$$

The first coefficients of the β-function in our conventions are given in appendix A.

Besides varying the scale μ_a at which the coupling constant is evaluated, in our numerical analysis we shall also use a different definition of the quark mass. Apart from the pole mass, the sum rules will also be analyzed in terms of a running $\overline{MS}$ mass $m(\mu_m)$, evaluated at a scale μ_m. Of course, physical quantities should remain unchanged. Therefore, the variation in our results originating from changes of scheme and scale in the coupling and quark mass will give an estimate of the uncertainty due to higher orders in perturbation theory. It should already be remarked that we have deliberately chosen different scales μ_a and μ_m in the coupling and mass respectively, in order to be able to vary them independently.

From the definition (1.3), it is easy to calculate the relations between the moments defined in terms of the pole mass and those expressed in terms of a running $\overline{MS}$ mass $m(\mu_m)$:

$$\overline{\mathcal{M}}_n^{(1)} \;=\; \mathcal{M}_n^{(1)} + 2n\, r_m^{(1)} \mathcal{M}_n^{(0)}\,, \tag{2.9}$$

$$\overline{\mathcal{M}}_n^{(2)} \;=\; \mathcal{M}_n^{(2)} + 2n\, r_m^{(1)} \mathcal{M}_n^{(1)} + n\Big(2r_m^{(2)} + (2n-1) r_m^{(1)^2}\Big) \mathcal{M}_n^{(0)}\,, \tag{2.10}$$

where $r_m^{(1)}$ and $r_m^{(2)}$ appear in the relation between pole and running $\overline{MS}$ mass

$$m(\mu_m) \;=\; M\left[\,1 + a(\mu_a)\, r_m^{(1)}(\mu_m) + a(\mu_a)^2\, r_m^{(2)}(\mu_a,\mu_m) + \dots\,\right]. \tag{2.11}$$

Explicit expressions for $r_m^{(1)}$ and $r_m^{(2)}$ are also given in appendix A.

As can be seen from table 1, for large n the higher-order corrections grow with respect to the leading order. At $n = 8$ the first order correction is roughly 120% of the leading term whereas the second order contribution is 140%. At $n = 20$ the contributions of first and second order are 200% and 340% respectively. This behaviour of the perturbation series for large moments is well known [17, 18, 25] and originates from the fact that the relevant parameter in the Coulomb system is α_s/v which leads to a $\alpha_s\sqrt{n}$ dependence of the moments. Thus for higher n the perturbative corrections become increasingly more important and have to be summed up explicitly in order for the theoretical expressions to make sense. This Coulomb resummation will be discussed in the next section.

If, on the other hand, the $\overline{MS}$ mass is used, it is not clear how a Coulomb resummation could be performed, because now the velocity v depends on the renormalization scale. However, the radiative corrections in the $\overline{MS}$ scheme are somewhat smaller than if a pole mass is used. At $\mu_a = \mu_m = m$ and $n = 8$ the first and second order corrections are -27% and 3% whereas for $n = 20$ they are -170% and 115% respectively. This suggests to try to find a scale μ_m for which the perturbative corrections stay within a reasonable range. If we require the second-order correction not to exceed 50%, the scale μ_m should lie within $2.7\,\mathrm{GeV} \lesssim \mu_m \lesssim 3.7\,\mathrm{GeV}$. For the numerical analysis it is therefore possible to also exploit the sum rules in the $\overline{MS}$ scheme if $\mu_m \approx 3.2 \pm 0.5\,\mathrm{GeV}$ is chosen.

3 Coulomb resummation

Let us first state our Ansatz for the Coloumb resummed spectral function $R(v)$ and then discuss the different components:

$$R(v) \;=\; \Big(1 - 4C_F a + 16C_F^2 a^2\Big)\Big\{\, R^{(0)} + R_C + \widetilde{R}^{(1)} a + \widetilde{R}^{(2)} a^2 \,\Big\}\,, \tag{3.1}$$

with

$$R_C \;=\; \frac{9}{2}\Big[\,\frac{x_V}{(1 - e^{-x_V/v})} - v\,\Big]\,, \tag{3.2}$$

$$\widetilde{R}^{(1)} \;=\; R^{(1)} + 4C_F R^{(0)} - \frac{9}{4}\,\pi^2 C_F\,, \tag{3.3}$$

$$\widetilde{R}^{(2)} \;=\; R^{(2)} + 4C_F R^{(1)} - \frac{3\pi^4 C_F^2}{8v} - \frac{9}{4}\,\pi^2 C_F\, r_V^{(1)}\,. \tag{3.4}$$

Here, $x_V \equiv \pi^2 C_F a_V$ and a_V is the effective coupling which corresponds to the heavy quark-antiquark potential. Expressed in terms of the $\overline{MS}$ coupling, we have

$$a_V(\vec{q}^{\,2}) \;=\; a(\mu_a)\,\Big[\,1 + a(\mu_a)\, r_V^{(1)}(\vec{q}^{\,2}/\mu_a^2) + a(\mu_a)^2\, r_V^{(2)}(\vec{q}^{\,2}/\mu_a^2) + \ldots\,\Big]\,. \tag{3.5}$$

Because a_V is related to the static QCD potential it is independent of the renormalization scale but it does depend on the three-momentum transfer between the heavy quark and antiquark. Explicit expressions for $r_V^{(1)}$ and $r_V^{(2)}$ are given in appendix B.

The term R_C corresponds to the resummed spectral function resulting from the imaginary part of the Green function for the QCD Coloumb potential. It

resums the leading $(a/v)^n$ and some of the sub-leading corrections [5]. The corresponding terms have to be subtracted from $R^{(1)}$ and $R^{(2)}$. Although the QCD corrections to R are only known to order a^2, we have included the recently calculated $\mathcal{O}(a^3)$ contribution for a_V [43,44], in order to investigate the dependence of our results on higher-order corrections. This will be discussed further in section 6. In addition, we have factored out the correction to the vector current which originates from transversal, hard gluons. To the known correction "$-4C_F a$" we have added a term $16C_F^2 a^2$ in order not to generate additional corrections of order a^2 proportional to $R^{(0)}$. We shall comment further on this point below. After performing the Coulomb resummation, the large-moment behaviour of the remaining terms is much weaker. Let us discuss the different contributions in more detail.

It should be clear from eq. (1.4) that the large-n behaviour can always be inferred from the small-v behaviour of $R(v)$. Expanding eq. (2.4), we obtain

$$\mathcal{M}_n^{(0)} \;=\; \frac{9\sqrt{\pi}}{4n^{3/2}}\left\{1-\frac{7}{2^3 n}+\frac{145}{2^7 n^2}-\frac{1645}{2^{10}n^3}+\mathcal{O}\Big(\frac{1}{n^4}\Big)\right\}. \tag{3.6}$$

The small-v expansion of $R^{(1)}$ is given by:

$$R^{(1)} \;=\; 3\pi^2-24v+2\pi^2v^2+\Big(16\ln(8v^2)-\frac{148}{3}\Big)v^3-\pi^2v^4+\mathcal{O}(v^5)\,. \tag{3.7}$$

The first two terms are canceled by the additional contributions to $\widetilde{R}^{(1)}$. Therefore, although $\mathcal{M}_n^{(1)}/\mathcal{M}_n^{(0)}$ increases as $\sqrt{n}$, now

$$\frac{\widetilde{\mathcal{M}}_n^{(1)}}{\mathcal{M}_n^{(0)}} \;=\; \frac{8\pi^{3/2}}{9\sqrt{n}}-\frac{16}{3n}\left[\ln\Big(\frac{n}{2}\Big)+\gamma_E+\frac{11}{12}\right]-\frac{\pi^{3/2}}{n^{3/2}}+\mathcal{O}\Big(\frac{1}{n^2}\Big)\,. \tag{3.8}$$

For the moments $n=8,\ldots,20$ the second term is of the same size as the first. Thus for the case of interest the large-n expansion is very badly behaved. In fact, below $n\approx 100$ the ratio $\widetilde{\mathcal{M}}_n^{(1)}/\mathcal{M}_n^{(0)}$ increases and only for $n>100$ the asymptotic $1/\sqrt{n}$ decrease is approached.

The available analytical results for $R_l^{(2)}$ and $R_F^{(2)}$ allow to calculate the small-v behaviour for these functions as well:

$$R_l^{(2)} \;=\; \frac{3\pi^2}{4}\Big[\ln\frac{4v^2}{(1-v^2)}-\frac{5}{3}\Big]+\frac{11}{2}v+\frac{\pi^2}{2}\Big[\ln\frac{4v^2}{(1-v^2)}-\frac{17}{3}\Big]v^2+\mathcal{O}(v^3)\,, \tag{3.9}$$

$$R_F^{(2)} \;=\; \Big(22-2\pi^2\Big)v-\Big(\frac{245}{18}-\frac{4\pi^2}{3}\Big)v^3+\mathcal{O}(v^4)\,. \tag{3.10}$$

Again, the first term in eq. (3.9) is canceled by the corresponding piece in the last term of eq. (3.4) if we substitute $\vec{q}^{\,2}=v^2s=4v^2M^2/(1-v^2)$ and if the first

coefficient of the β-function in $r_V^{(1)}$ is evaluated with n_l light quark flavours. On the other hand, $R_F^{(2)}$ vanishes at threshold and hence has no contribution which should be resummed in the Coulomb term. This indicates that consistently the coupling constant in R_C should be evaluated in an effective theory with only n_l active flavours. To facilitate the numerical analysis, we then prefer to rewrite the full expression for $\mathcal{M}_n$ in terms of the coupling a defined in the n_l-flavour theory. From the matching relations for a [45–47], it follows that this just amounts to using the corresponding β_1 with n_l flavours in eq. (2.8).

Analogously, all terms of $\mathcal{O}(1/v)$, $\mathcal{O}(\ln v^2)$ and $\mathcal{O}(1)$ for $R_A^{(2)}$ and $R_{NA}^{(2)}$ are canceled in eq. (3.4), such that $\widetilde{R}^{(2)}$ vanishes in the limit $v \to 0$. Nevertheless, for these two functions the contributions of $\mathcal{O}(v)$ which determine the constant terms in $\widetilde{\mathcal{M}}_{n,A}^{(2)}/\mathcal{M}_n^{(0)}$ and $\widetilde{\mathcal{M}}_{n,NA}^{(2)}/\mathcal{M}_n^{(0)}$ are not known analytically. Precisely those terms correspond to the current correction from transversal, hard gluons. In order to obtain information on the large-n behaviour of the second-order moments, we can assume an expansion analogous to eq. (3.8), however including a constant term and fitting this Ansatz to the moments as calculated from the Padé approximation. We then find

$$\frac{\widetilde{\mathcal{M}}_n^{(2)}}{\mathcal{M}_n^{(0)}} \;\approx\; 161.1 - \frac{1174.3}{\sqrt{n}} + 819.9\,\frac{\ln n}{n} + \frac{534.6}{n} + \ldots\,. \tag{3.11}$$

The fit has been determined using moments with $n = 20, \ldots, 50$, but the coefficients are rather stable if the number of fit points is changed. Although the error on the coefficients probably is substantial, it nevertheless shows that again here the large-n expansion converges slowly and for the range of n in which we are interested, higher-order terms have to be included.

From the constant term in eq. (3.11), we can in principle infer the short distance correction resulting from transversal gluons. However, in the region of interest, namely for $n = 8, \ldots, 20$, the ratio $\widetilde{\mathcal{M}}_n^{(2)}/\mathcal{M}_n^{(0)} \approx 40$. This contribution should be added to the $16C_F^2$ already factorized in eq. (3.1), therefore further increasing this positive correction. In the work by Voloshin [24], the BLM scale setting prescription [26] was applied to absorb the $\mathcal{O}(a^2)$ correction in the term $-4C_F\,a(\mu_a)$ by changing the renormalization scale μ_a, and it was found that this should be accomplished with the choice $\mu_a \approx 0.63 M_b$. Because the first and second order terms appear with different signs, from the explicit calculation we now see that on the contrary the scale μ_a should be greater than M_b. Because we keep the $\mathcal{O}(a^2)$ correction explicitly, there is no need to evaluate this scale here.

4 Gluon condensate

Analytical results for the gluon condensate contribution to the massive vector correlator are available at the next-to-leading order [4,48]. Adopting the notation of ref. [48], the corresponding moments are given by

$$\mathcal{M}_{n,G^2} \;=\; \frac{3\pi^2}{4}\,\frac{\langle aGG\rangle}{M^4}\,a_n^V\Big[\,1+a\,b_n^V\,\Big]\,, \tag{4.1}$$

with

$$a_n^V \;=\; -\,\frac{1}{24}\,(n+1)(n+3)B(1/2,n+3)\,, \tag{4.2}$$

and the coefficients b_n^V together with numerical values for the a_n^V up to $n=21$ are shown in table 2. The coefficients b_n^V depend on the renormalization scheme for the mass. If the $\overline{MS}$ scheme is used the b_n^V change according to

$$\overline{b}_n^V \;=\; b_n^V + (2n+4)\,r_m^{(1)}\,. \tag{4.3}$$

n	1	2	3	4	5	6	7
a_n^V	-0.3048	-0.5079	-0.7388	-0.9946	-1.2730	-1.5726	-1.8918
b_n^V	10.4768	11.7202	12.8494	13.8928	14.8685	15.7888	16.6625
n	8	9	10	11	12	13	14
a_n^V	-2.2296	-2.5851	-2.9574	-3.3457	-3.7495	-4.1682	-4.6012
b_n^V	17.4964	18.2956	19.0643	19.8058	20.5229	21.2179	21.8928
n	15	16	17	18	19	20	21
a_n^V	-5.0482	-5.5087	-5.9823	-6.4686	-6.9674	-7.4784	-8.0012
b_n^V	22.5492	23.1887	23.8124	24.4216	25.0173	25.6002	26.1712

Table 2: First- and second-order coefficients for the gluon condensate contribution to the moments $\mathcal{M}_n$.

From eq. (4.2) it is clear that the relative growth of $\mathcal{M}^{(0)}_{n,G^2}/\mathcal{M}^{(0)}_n$ is proportional to n^3. Therefore, the non-perturbative contribution grows much faster than the perturbative moments. In addition, as can be seen from table 2, in the pole-mass scheme at $\mu_a = M$ the next-to-leading order correction is of the same size or larger as the leading term. Because the perturbative expansion for the gluon condensate cannot be trusted, we shall restrict our analysis to a range of n where its contribution to the moments is small and can be neglected. Using

$\langle aGG \rangle \approx 0.021\,\mathrm{GeV}^4$ [48, 49], we find that for $n \leq 20$ the contribution from the gluon condensate to the $b\bar{b}$ moments is below 3%. Thus, we shall restrict our phenomenological analysis to this range.

In the $\overline{MS}$ scheme the situation concerning the perturbative expansion is somewhat better. If we take $\mu_m \approx 3.2\,\mathrm{GeV}$, as was discussed at the end of section 2, for $n \leq 20$ the next-to-leading order contribution stays below 70% of the leading order. This demonstrates that a determination of the gluon condensate from charmonium should be performed in the $\overline{MS}$ scheme. Nevertheless, for this work also in the $\overline{MS}$ scheme we shall keep the restriction to $n \leq 20$. A lower limit on the number of moments will be discussed in the next section.

5 Phenomenological parameterization

In the preceding sections, theoretical predictions for the spectral function $R(s)$ and the related moments $\mathcal{M}_n$ have been calculated without further specifying the actual quark content. For the phenomenological parameterization of the spectral function we shall now restrict our discussion to the $b\bar{b}$ system.

In the narrow-width approximation the contribution to $R_b(s)$ from a $\Upsilon(kS)$ resonance is given by

$$R_{b,kS}(s) \;=\; \frac{9\pi}{\bar{\alpha}^2}\,\Gamma(\Upsilon(kS) \to e^+e^-)\,M_{kS}\,\delta(s - M_{kS}^2)\,, \tag{5.1}$$

where $\bar{\alpha}$ denotes the running QED coupling evaluated at a scale around the resonance mass. Because in the Review of Particle Properties [50] the electronic widths have been calculated with $\bar{\alpha}^2 = 1.07\,\alpha^2$ where $\alpha = 1/137.04$ is the fine structure constant, we shall use this value accordingly. In the case at hand the narrow-width approximation is extremely good because the full widths of the first three Υ resonances are roughly a factor 10^{-5} smaller than the corresponding masses and the higher-resonance contributions to the moments are suppressed.

Experimentally, the first six resonances have been observed. The measured masses and electronic widths are collected in table 3. For our numerical analysis the errors on the masses can be safely neglected and have thus not been listed. Inserting eq. (5.1) in the definition of the moments $\mathcal{M}_n$, eq. (1.3), we obtain

$$\mathcal{M}_n \;=\; (4M_b^2)^n \left\{ \frac{9\pi}{\bar{\alpha}^2 Q_b^2} \sum_{k=1}^{6} \frac{\Gamma_{kS}}{M_{kS}^{2n+1}} + \int\limits_{s_0}^{\infty} ds\, \frac{R^{pt}(s)}{s^{n+1}} \right\}. \tag{5.2}$$

k	1	2	3	4	5	6
M_{kS} [GeV]	9.460	10.023	10.355	10.580	10.865	11.019
Γ_{kS} [keV]	1.31 ± 0.04	0.52 ± 0.03	0.48 ± 0.08	0.25 ± 0.03	0.31 ± 0.07	0.13 ± 0.03

Table 3: Masses and electronic widths of the first six $\Upsilon(kS)$ resonances.

The numerical weight of the heavier resonances in (5.2) decreases strongly for increasing values of n. The contribution of the $\Upsilon(5S)$ [$\Upsilon(6S)$] state is 9.5% [4%] at $n = 0$; 1% [0.3%] at $n = 10$; and a tiny 0.08% [0.02%] at $n = 20$. Therefore, taking $n \gtrsim 10$, the uncertainties associated with the contributions of higher-mass states are very small.

The second term in eq. (5.2) accounts for the contributions to R_b above the sixth resonance and is approximated by the perturbative continuum. Generally, the continuum threshold $\sqrt{s_0}$ should lie around the mass of the next resonance, which has been estimated in potential models [51]. For our analysis we shall use $\sqrt{s_0} = 11.2 \pm 0.2\,\text{GeV}$. The lower value for s_0 includes the mass of the sixth resonance and should be a conservative estimate. There is still a contribution missing which stems from open B production above the $B\bar{B}$ threshold and below s_0. From the experimental data [52] we infer that its influence is small and has been included in the variation of s_0.

6 Numerical analysis in the pole-mass scheme

Quark-hadron duality entails the equality of the theoretical moments $\mathcal{M}_n^{th}$ presented in sections 2 to 4 and the phenomenological moments $\mathcal{M}_n^{ph}$ discussed in the previous section. The moments corresponding to the Coulomb term R_C of eq. (3.2) have been calculated from eq. (1.4) by numerical integration. To suppress higher resonances as well as power corrections, following ref. [24], we have restricted n to the range $n = 8, \ldots, 20$. Solving the moment sum rules for M_b, we can fit M_b to a constant by varying M_b and $\alpha_s(M_b)$. The fit has been performed using the program Minuit [53]. For the central set of parameter values our result is

$$M_b = 4.604 \pm 0.009\ \text{GeV}\,, \tag{6.1}$$

$$\alpha_s(M_b) = 0.2197 \pm 0.0097\,. \tag{6.2}$$

The error in these results just corresponds to the statistical error of the fit. In the fit we have included every second moment to have less statistical dependence, but the results change very little if all moments with $n = 8, \ldots, 20$ or only every fourth moment is used. In figure 1 the resulting values for M_b are displayed as a function of n. This illustrates that a constant M_b in the range $8 \leq n \leq 20$ really produces an excellent fit.

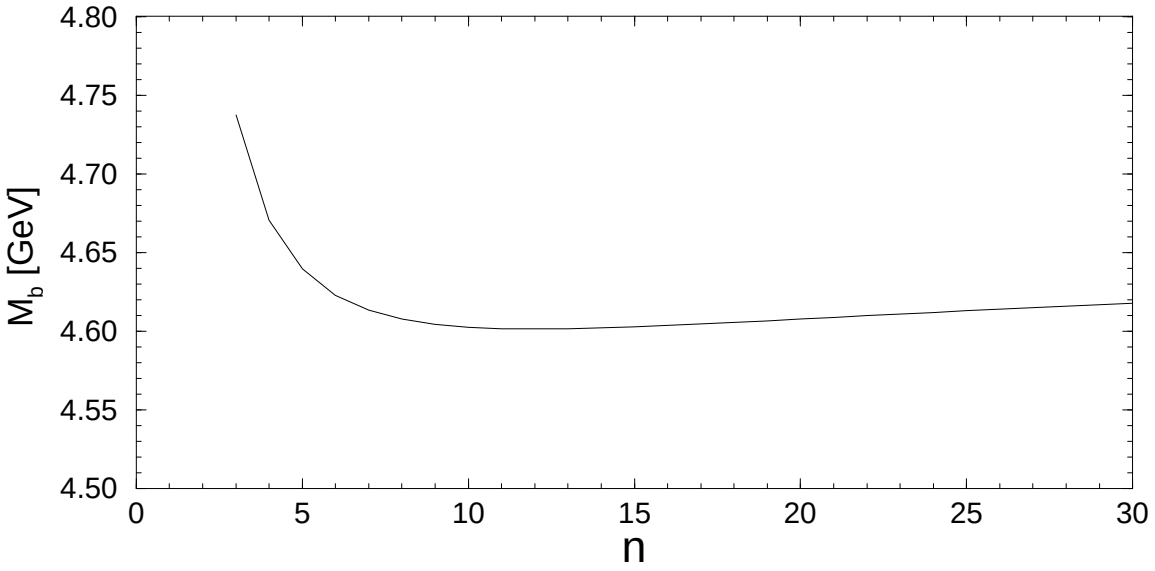

Figure 1: The b quark pole mass as a function of n.

In the remaining part of this section let us present a detailed discussion of the errors resulting from the various input quantities. A compilation of all different contributions to the errors on M_b and $\alpha_s(M_b)$ is summarized in table 4. The dominant theoretical uncertainty is due to the unknown higher-order perturbative corrections. We have estimated this uncertainty in three different ways. As has been already remarked in section 3 the relation between the effective coupling a_V in the Coulomb potential and $a^{\overline{MS}}$ is known to $\mathcal{O}(a^3)$ [43, 44]. We can thus include this correction in R_C to see what the influence on our results is. Although this is not consistent because the corresponding correction $\widetilde{R}^{(3)}$ is not available, it nevertheless can be taken as an error estimate of higher-order corrections. A second possibility is a variation of the scale at which α_s is evaluated. For the result in table 4 we have chosen the range $M_b/2 \leq \mu_a \leq 2M_b$. As a final test on the importance of higher-order corrections, we can remove the $\mathcal{O}(a^2)$ term $\widetilde{R}^{(2)}$

	ΔM_b [MeV]	$\Delta\alpha_s(M_b)$ [10^{-3}]
statistical	± 9.1	± 9.7
$\mathcal{O}(a^3)$ Coulomb	± 7.3	± 22.2
$\mathcal{O}(a^2)$	± 0.9	± 8.2
scale μ_a	$\pm^{2.1}_{1.3}$	$\pm^{28.7}_{19.6}$
continuum	$\pm^{2.6}_{2.0}$	$\pm^{3.7}_{2.7}$
$\langle aGG\rangle$	± 5.3	± 3.6
$\Gamma_{e^+e^-}$	± 3.1	± 6.7
total	± 13.5	± 26.9

Table 4: Separate contributions to the errors of M_b and $\alpha_s(M_b)$.

completely. From table 4 we observe that including the $\mathcal{O}(a^3)$ correction to a_V has a much bigger influence than removing $\widetilde{R}^{(2)}$. This is not unexpected because the Coulomb piece sums up the dominant contributions in the large-n limit. The uncertainty of the scale dependence is of the same order as the sum of the other two contributions. For our estimate of the uncertainty resulting from higher-order corrections we can now either take the scale dependence or combine the other two contributions. Adding all three would double count the error, because the uncertainty in an asymptotic series, such as the perturbative expansion, is bounded by the size of the last known term. For our final results, we have chosen to include the errors of varying the Coulomb and the $\mathcal{O}(a^2)$ terms.

The error from the continuum contribution has been estimated by varying s_0 in the range $\sqrt{s_0} = 11.2 \pm 0.2\,\text{GeV}$. The entry for the gluon condensate in table 4 results from removing the gluon condensate completely and for the uncertainty from the electronic widths we have varied all widths within the errors given in table 3. With respect to the uncertainty resulting from higher orders all these errors are small. Adding all errors in quadrature, we arrive at our final result in the pole-mass scheme:

$$M_b = 4.604 \pm 0.014\ \text{GeV}\,, \tag{6.3}$$

$$\alpha_s(M_b) = 0.2197 \pm 0.0269\,. \tag{6.4}$$

Evolving the strong coupling constant to M_Z, we find

$$\alpha_s(M_Z) = 0.1184 \pm^{0.0070}_{0.0080}\,. \tag{6.5}$$

Our central result is in astonishingly good agreement to the current world average [36], although the error turns out to be larger. Further comments on our results also with respect to the paper by Voloshin [24] have been relegated to the conclusions.

7 Numerical analysis in the $\overline{MS}$ scheme

Besides analyzing the moment sum rules exploiting the pole mass M_b, in addition we have investigated the same sum rules in the $\overline{MS}$ scheme. In contrast to the pole mass, the quark mass in the $\overline{MS}$ scheme depends on the renormalization scale μ_m. As has been remarked in section 2, to restrict the $\mathcal{O}(a^2)$ corrections to a reasonable size, μ_m should lie in the range $\mu_m = 3.2 \pm 0.5\,\mathrm{GeV}$. We have refrained from performing a resummation of the large radiative corrections because now the velocity v depends on the renormalization scheme and it is not straightforwardly possible to proceed in analogy to the Coulomb resummation for the pole mass.

The fitting procedure was performed along the same lines as for the pole-mass case. For the central values of our input parameters, we obtain

$$m_b(m_b) = 4.133 \pm 0.002\ \mathrm{GeV}\,, \tag{7.1}$$

$$\alpha_s(m_b) = 0.2325 \pm 0.0044\,, \tag{7.2}$$

where again the errors are purely statistical. Since it is more standard to evaluate the running b-quark mass at m_b, we have evolved our immediate result $m_b(3.2\,\mathrm{GeV})$ to this scale with the help of the renormalization group equation.

	Δm_b [MeV]	$\Delta\alpha_s(m_b)$ $[10^{-3}]$
statistical	± 2	± 4.4
scale μ_m	$\pm^{33}_{36}$	$\pm^{36.2}_{5.8}$
scale μ_a	$\pm^{49}_{31}$	$\pm^{25.1}_{28.0}$
continuum	± 1	$\pm^{3.5}_{2.6}$
$\langle aGG\rangle$	± 2	± 2.3
$\Gamma_{e^+e^-}$	± 3	± 6.0
total	$\pm^{59}_{48}$	$\pm^{44.9}_{29.7}$

Table 5: Separate contributions to the errors of $m_b(m_b)$ and $\alpha_s(m_b)$.

The separate contributions to the theoretical error have been obtained by performing the same variations as for the pole-mass scheme and have been listed in table 5. The uncertainty from higher-order corrections is now due to the variation of the scales $\mu_m = 3.2 \pm 0.5\,\text{GeV}$ and $2.6\,\text{GeV} \leq \mu_a \leq 2m_b$. The scale μ_a should not be taken lower than roughly 2.6 GeV because otherwise the $\mathcal{O}(a^2)$ correction $\overline{\mathcal{M}}_n^{(2)}$ becomes unacceptably large. Since in addition to μ_a for the $\overline{MS}$ scheme we can also vary μ_m, the resulting uncertainty, especially for m_b, is larger than for the pole mass. Adding all errors in quadrature, we arrive at our final result in the $\overline{MS}$ scheme:

$$m_b(m_b) = 4.13 \pm 0.06\ \text{GeV}\,, \tag{7.3}$$

$$\alpha_s(m_b) = 0.2325 \pm {}^{0.0449}_{0.0297}\ . \tag{7.4}$$

Evolving the strong coupling constant to M_Z, we find

$$\alpha_s(M_Z) = 0.1196 \pm {}^{0.0102}_{0.0080}\ . \tag{7.5}$$

It is gratifying to observe that the resulting values for $\alpha_s(M_Z)$ from the pole-mass and $\overline{MS}$ schemes turn out to be in very good agreement. This is a further indication that the uncertainty from unknown higher-order corrections is under control. In addition, our results $m_b(m_b)$ and M_b for the b-quark mass satisfy the relation (A.4) between the pole and $\overline{MS}$ mass within the errors. This should be expected because the relation (A.4) has been used to rewrite the moment sum rules in terms of the $\overline{MS}$ mass. Nevertheless, it again shows that variations due to higher orders are accounted for by our error estimates.

8 Conclusions

Before we enter a discussion of our findings, let us again summarize the central results. For the bottom quark mass in the pole-mass as well as $\overline{MS}$ scheme, we obtain

$$M_b = 4.60 \pm 0.02\ \text{GeV}\,, \tag{8.1}$$

$$m_b(m_b) = 4.13 \pm 0.06\ \text{GeV}\,, \tag{8.2}$$

respectively. Combining both determinations of the strong coupling constant α_s, we find

$$\alpha_s(M_Z) = 0.119 \pm 0.008\,. \tag{8.3}$$

We have not averaged the errors of the two determinations because they are not independent.

The bottom quark mass values obtained by us are in good agreement to previous determinations from QCD sum rules [22, 23, 54–56] and a very recent calculation from lattice QCD [57]. Owing to the big sensitivity of the moment sum rules for the Υ system to the quark mass, and the good control over higher-order α_s corrections, our result is more precise.

Nevertheless, the pole quark-mass value obtained by us is in disagreement to the result found by Voloshin [24]. In our opinion the discrepancy is due to the importance of higher $\mathcal{O}(1/n)$ corrections, which in ref. [24] were either neglected, or numerically fitted from the sum rules. In [24] it was assumed that the leading order correction goes like $1/n$. However, from eqs. (3.8) and (3.11), it is clear that they rather behave like $1/\sqrt{n}$. Besides, we have also demonstrated that for the region of n used in the analysis, the large-n expansion is not justified. In addition, the second-order α_s correction was only partially and partly incorrectly taken into account. Therefore, the scale dependence of α_s was not under control.

Let us shortly comment on the renormalon ambiguity of the pole mass. During the last years, it has been realized that beyond perturbation theory the pole masses for the charm and bottom quarks suffer from unknown renormalon ambiguities, leading to additional theoretical uncertainties in their determination [58–60]. On general grounds this uncertainty has been estimated to be of $\mathcal{O}(100\,\mathrm{MeV})$. Throughout our analysis, the pole mass has been defined as the pole of the perturbatively renormalized quark propagator. Our determination (8.1) might therefore be subject to additional uncertainties which go beyond perturbation theory but which we cannot assess in a precise way.

Within our errors the result obtained for $\alpha_s(M_Z)$, eq. (8.3), is compatible with the result by Voloshin [24], though, given the shortcomings of this analysis discussed above, his errors appear to be largely underestimated. Thus, previous claims of a low value of $\alpha_s(M_Z)$ from low-energy determinations which could hint to new physics [24, 37] are unfounded. On the other hand, our central value for $\alpha_s(M_Z)$ is surprisingly close to the current world average $\alpha_s(M_Z) = 0.118 \pm 0.003$ [36], although the error is certainly larger.

The dominant uncertainty for the determination of the b-quark mass and α_s from the Υ system was found to originate from the dependence on the renormalization scale, or, equivalently, the size of the as yet unknown higher-order corrections. Improving the error on the α_s determination will thus only be possi-

ble if the full $\mathcal{O}(\alpha_s^3)$ correction to the moments $\mathcal{M}_n$ is known and if it turns out to be reasonably small. We hope to return to this question in the future.

Acknowledgments

M. J. would like to thank H. G. Dosch and D. Gromes for helpful discussions. This work has been supported in part by the German–Spanish Cooperation agreement HA95-0169. The work of A.P. has been supported in part by CICYT (Spain) under the grant AEN-96-1718.

Appendices

A Renormalization group functions

For the definition of the renormalization group functions we follow the notation of Pascual and Tarrach [61], except that we define the β-function such that β_1 is positive. The expansions of $\beta(a)$ and $\gamma(a)$ take the form:

$$\beta(a) \;=\; -\beta_1 a - \beta_2 a^2 - \beta_3 a^3 - \ldots\,, \quad \text{and} \quad \gamma(a) \;=\; \gamma_1 a + \gamma_2 a^2 + \gamma_3 a^3 + \ldots\,, \tag{A.1}$$

with

$$\beta_1 \;=\; \frac{1}{6}\Big[\,11C_A - 4Tn_f\,\Big]\,, \qquad \beta_2 \;=\; \frac{1}{12}\Big[\,17C_A^2 - 10C_ATn_f - 6C_FTn_f\,\Big]\,, \tag{A.2}$$

and

$$\gamma_1 \;=\; \frac{3}{2}\,C_F\,, \qquad \gamma_2 \;=\; \frac{C_F}{48}\Big[\,97C_A + 9C_F - 20Tn_f\,\Big]\,. \tag{A.3}$$

The relation between pole and running $\overline{MS}$ mass is given by

$$m(\mu_m) \;=\; M\Big[\,1 + a(\mu_a)\,r_m^{(1)}(\mu_m) + a(\mu_a)^2\,r_m^{(2)}(\mu_a,\mu_m) + \ldots\,\Big]\,, \tag{A.4}$$

where

$$r_m^{(1)} \;=\; r_{m,0}^{(1)} - \gamma_1 \ln\frac{\mu_m}{m(\mu_m)}\,, \tag{A.5}$$

$$\begin{aligned} r_m^{(2)} \;=\;& r_{m,0}^{(2)} - \Big[\,\gamma_2 + (\gamma_1-\beta_1)\,r_{m,0}^{(1)}\,\Big]\ln\frac{\mu_m}{m(\mu_m)} + \frac{\gamma_1}{2}\,(\gamma_1-\beta_1)\ln^2\frac{\mu_m}{m(\mu_m)} \\ & - \Big[\,\gamma_1 + \beta_1\ln\frac{\mu_m}{\mu_a}\,\Big]r_m^{(1)}\,. \end{aligned} \tag{A.6}$$

The coefficients of the logarithms can be calculated from the renormalization group and the constant coefficients $r_{m,0}^{(1)}$ and $r_{m,0}^{(2)}$ are found to be [29, 62, 63]

$$r_{m,0}^{(1)} \;=\; -\,C_F\,, \tag{A.7}$$

$$\begin{aligned} r_{m,0}^{(2)} \;=\;& C_F^2\Big(\frac{7}{128} - \frac{15}{8}\zeta(2) - \frac{3}{4}\zeta(3) + 3\zeta(2)\ln 2\Big) + C_FTn_f\Big(\frac{71}{96} + \frac{1}{2}\zeta(2)\Big) \\ & + C_AC_F\Big(-\frac{1111}{384} + \frac{1}{2}\zeta(2) + \frac{3}{8}\zeta(3) - \frac{3}{2}\zeta(2)\ln 2\Big) + C_FT\Big(\frac{3}{4} - \frac{3}{2}\zeta(2)\Big)\,. \end{aligned} \tag{A.8}$$

B The effective coupling a_V

In terms of the $\overline{MS}$ coupling the effective coupling a_V is given by

$$a_V(\vec{q}^{\,2}) \;=\; a(\mu_a)\Big[\,1 + a(\mu_a)\,r_V^{(1)}(\vec{q}^{\,2}/\mu_a^2) + a(\mu_a)^2\,r_V^{(2)}(\vec{q}^{\,2}/\mu_a^2) + \ldots\,\Big]\,, \tag{B.1}$$

where

$$r_V^{(1)} \;=\; r_{V,0}^{(1)} - \frac{\beta_1}{2}\ln\frac{\vec{q}^{\,2}}{\mu_a^2}\,, \tag{B.2}$$

$$r_V^{(2)} \;=\; r_{V,0}^{(2)} - \Big[\,\frac{\beta_2}{2} + \beta_1 r_{V,0}^{(1)}\Big]\ln\frac{\vec{q}^{\,2}}{\mu_a^2} + \frac{\beta_1^2}{4}\ln^2\frac{\vec{q}^{\,2}}{\mu_a^2}\,. \tag{B.3}$$

Like in eq. (A.4) the coefficients of the logarithms are determined by the renormalization group and the constant coefficients $r_{V,0}^{(1)}$ and $r_{V,0}^{(2)}$ are found to be [43, 44, 64, 65]

$$r_{V,0}^{(1)} \;=\; \frac{31}{36}\,C_A - \frac{5}{9}\,Tn_l\,, \tag{B.4}$$

$$\begin{aligned} r_{V,0}^{(2)} \;=\; & \frac{1}{16}\Bigg\{ C_A^2\Big(\frac{4343}{162} + 6\pi^2 - \frac{\pi^4}{4} + \frac{22}{3}\zeta(3)\Big) - C_A T n_l\Big(\frac{1798}{81} + \frac{56}{3}\zeta(3)\Big) \\ & - C_F T n_l\Big(\frac{55}{3} - 16\zeta(3)\Big) + T^2 n_l^2\,\frac{400}{81}\Bigg\}\,. \end{aligned} \tag{B.5}$$

Here, $n_l = n_f - 1$ is the number of light quark flavours.

References

[1] W. Buchmüller, G. Grunberg, and S. H.-H. Tye, *Phys. Rev. Lett.* **45** (1980) 103.

[2] W. Buchmüller and S. H.-H. Tye, *Phys. Rev.* **D24** (1981) 132.

[3] A. Martin, *Phys. Lett.* **100B** (1981) 511.

[4] M. A. Shifman, A. I. Vainshtein, and V. I. Zakharov, *Nucl. Phys.* **B147** (1979) 385, 448, 519.

[5] M. B. Voloshin, *Nucl. Phys.* **B154** (1979) 365.

[6] H. Leutwyler, *Phys. Lett.* **B98** (1981) 447.

[7] M. B. Voloshin, *Yad. Fiz.* **36** (1982) 247.

[8] J. S. Bell and R. A. Bertlmann, *Nucl. Phys.* **B227** (1983) 435.

[9] H. G. Dosch, *Phys. Lett.* **B190** (1987) 177.

[10] A. Krämer, H. G. Dosch, and R. A. Bertlmann, *Phys. Lett.* **B223** (1989) 105.

[11] A. Krämer, H. G. Dosch, and R. A. Bertlmann, *Fortschr. Phys.* **40** (1992) 93.

[12] S. Titard and F. J. Ynduráin, *Phys. Rev.* **D49** (1994) 6007.

[13] S. Titard and F. J. Ynduráin, *Phys. Rev.* **D51** (1995) 6348.

[14] S. Titard and F. J. Ynduráin, *Phys. Lett.* **B351** (1995) 541.

[15] Y. A. Simonov, S. Titard, and F. J. Ynduráin, *Phys. Lett.* **B354** (1995) 435.

[16] W. A. Bardeen, A. J. Buras, D. W. Duke, and T. Muta, *Phys. Rev.* **D18** (1978) 3998.

[17] V. A. Novikov et al., *Phys. Rev. Lett.* **38** (1977) 626.

[18] V. A. Novikov et al., *Phys. Rep.* **C41** (1978) 1.

[19] S. S. Grigorian, *Sov. J. Nucl. Phys.* **30** (1979) 729.

[20] J. S. Bell and R. A. Bertlmann, *Nucl. Phys.* **B177** (1981) 218.

[21] B. Guberina, R. Meckbach, R. D. Peccei, and R. Rückl, *Nucl. Phys.* **B184** (1981) 476.

[22] L. J. Reinders, H. Rubinstein, and S. Yazaki, *Nucl. Phys.* **B186** (1981) 109.

[23] L. J. Reinders, H. Rubinstein, and S. Yazaki, *Phys. Rep.* **127** (1985) 1.

[24] M. B. Voloshin, *Int. J. Mod. Phys.* **A10** (1995) 2865.

[25] M. B. Voloshin and Y. M. Zaitsev, *Sov. Phys. Usp.* **30** (1987) 553.

[26] S. Brodsky, G. Lepage, and P. Mackenzie, *Phys. Rev.* **D28** (1983) 228.

[27] P. A. Baikov and D. J. Broadhurst, *New Computing Techniques in Physics Research IV*, Pisa Workshop, World Scientific, 1995.

[28] K. G. Chetyrkin, J. H. Kühn, and M. Steinhauser, *Phys. Lett.* **B371** (1996) 93.

[29] K. G. Chetyrkin, J. H. Kühn, and M. Steinhauser, *Nucl. Phys.* **B482** (1996) 213.

[30] A. H. Hoang, J. H. Kühn, and T. Teubner, *Nucl. Phys.* **B452** (1995) 173.

[31] K. G. Chetyrkin, A. H. Hoang, J. H. Kühn, and M. Steinhauser, *Phys. Lett.* **B384** (1996) 233.

[32] E. Braaten, S. Narison, and A. Pich, *Nucl. Phys.* **B373** (1992) 581.

[33] A. Pich, *Nucl. Phys. Proc. Suppl.* **39B,C** (1995) 326.

[34] A. Pich, *Tau Lepton Physics: Theory Overview*, Proc. Fourth Workshop on Tau Lepton Physics (Colorado, September 1996) **hep-ph/9612308** (1996).

[35] A. Pich, *QCD Test from Tau Decays*, Proc. 20th Johns Hopkins Workshop on Non-Perturbative Particle Theory and Experimental Tests (Heidelberg, June 1996) **hep-ph/9701305** (1997).

[36] M. Schmelling, *talk given at XXVIII Int. Conf. on High Energy Physics, Warsaw, July 1996* **hep-ex/9701002** (1997).

[37] M. A. Shifman, *Int. J. Mod. Phys.* **A11** (1996) 3195.

[38] G. Källén and A. Sabry, *Dan. Vidensk. Selsk. Mat.-Fys. Medd.* **29** (1955) No. 17.

[39] J. Schwinger, *Particles, Sources and Fields, Vol. II*, Addison-Wesley, New York, 1973.

[40] S. C. Generalis, *Ph.D. thesis*, The Open University, Milton Keynes, England, 1984, (unpublished).

[41] D. J. Broadhurst, J. Fleischer, and O. V. Tarasov, *Z. Phys* **C 60** (1993) 287.

[42] L. Lewin, *Polylogarithms and Associated Functions*, North Holland, 1981.

[43] M. Peter, *Phys. Rev. Lett.* **78** (1997) 602.

[44] M. Peter, *Karlsruhe preprint* **TTP-97-03, hep-ph/9702245** (1997).

[45] W. Bernreuther and W. Wetzel, *Nucl. Phys.* **B197** (1982) 228.

[46] W. Bernreuther, *Annals of Phys.* **151** (1983) 127.

[47] S. A. Larin, T. van Ritbergen, and J. A. M. Vermaseren, *Nucl. Phys.* **B438** (1995) 278.

[48] D. J. Broadhurst et al., *Phys. Lett.* **B329** (1994) 103.

[49] S. Narison, *Phys. Lett.* **B387** (1996) 162.

[50] Particle Data Group, Review of Particle Properties, *Phys. Rev.* **D54** (1996).

[51] D. B. Lichtenberg, R. Roncaglia, J. G. Wills, and E. Pedrazzi, *Z. Phys.* **C47** (1990) 83.

[52] CLEO II Colaboration, *Phys. Rev. Lett.* **67** (1991) 1692.

[53] F. James, *Minuit Reference Manual* **D506** (1994).

[54] S. Narison, *QCD Spectral Sum Rules*, World Scientific Lecture Notes in Physics – Vol. **26**, 1989.

[55] C. A. Dominguez and N. Paver, *Phys. Lett.* **B293** (1992) 197.

[56] S. Narison, *Phys. Lett.* **B341** (1994) 73.

[57] V. Giménez, G. Martinelli, and C. T. Sachrajda, *CERN preprint* **CERN-TH/96-163, hep-lat/9607018** (1996).

[58] M. Beneke and V. M. Braun, *Nucl. Phys.* **B426** (1994) 301.

[59] I. I. Bigi, M. A. Shifman, N. G. Uraltsev, and A. I. Vainshtein, *Phys. Rev.* **D50** (1994) 2234.

[60] M. Neubert and S. Sachrajda, *Nucl. Phys.* **B438** (1994) 235.

[61] P. Pascual and R. Tarrach, *QCD: Renormalization for the Practitioner*, Lecture Notes in Physics **194**, Springer-Verlag, 1984.

[62] R. Tarrach, *Nucl. Phys.* **B183** (1981) 384.

[63] N. Gray, D. J. Broadhurst, W. Grafe, and K. Schilcher, *Z. Phys.* **C48** (1990) 673.

[64] W. Fischler, *Nucl. Phys.* **B129** (1977) 157.

[65] A. Billoire, *Phys. Lett.* **B92** (1980) 343.